Automatic Detection and Elimination of Specular Reflectance in Color Images by Means of MS Diagram and Vector Connected Filters

Francisco Ortiz and Fernando Torres, *Member, IEEE*

***Abstract*—This paper proposes a new method for the detection and elimination of specular reflectance in color images of real scenes. We use a two-dimensional histogram that allows us to relate the signals of intensity and saturation of a color image, and to identify the specularities in an area of the histogram. This is known as the Intensity-Saturation (MS) diagram, and it is constructed from the Intensity-Saturation-Hue (MSH) generalized color space. An experimental and detailed study of the presence of specularities in the MS diagram for different types of materials in real scenes is carried out. To eliminate the specularities detected, we use a new connected vectorial filter based on the extension of mathematical morphology to color images, employing a lexicographical order. This new filter operates only in the bright areas previously detected, avoiding the high cost of processing the connected filters and the related oversimplification. The proposed method achieves results similar to current methods, but without the need for costly multiple-view systems or stereo images.**

***Index Terms*—Brightness detection, brightness elimination, color mathematical morphology, connected vectorial filters, Intensity-Saturation (MS) diagram.**

I. Introduction

IN INDUSTRIAL visual inspection systems, images are acquired in work environments where the illumination plays an important role. Sometimes a bad adjustment of illumination can introduce brightness (highlights or specular reflectance) in the objects captured by the vision system. The presence of such brightness alters the pattern recognition process because the previous stage of detection of edges in the objects fails. As such, the correct identification of objects, a goal in computer vision, is difficult to realize.

The elimination of specular reflections is not only interesting in visual inspection, but also in other fields of computer vision, restoration, and reproduction of images, since the brightness affects the visual quality of the scene. There is no commercial software application that allows the automatic elimination of such specularities.

To be able to attenuate the effect of the specular reflectance in the captured scene, the phenomenon in the image must first be detected and identified. The dichromatic reflection model proposed by Safer [1] is a tool that has been used in many methods for detecting specularities. Such a model supposes that the interaction between the light and a dielectric material produces different spectral distributions in the object; i.e., the specular and diffuse reflectances. Diffuse component is a product of illumination and surface pigments, whereas specular reflectance has the same spectral makeup as its incident illuminant. The color of a given pixel in an image is a linear combination of a function of diffuse reflection and a function of specular reflection.

Based on this model, Lin *et al.* [2] have developed a system for eliminating specularities in image sequences by means of stereo correspondence. Bajcsy *et al.* [3] use a chromatic space based on polar coordinates that allows the detection of specular and diffuse reflections by means of the previous knowledge of the captured scene. Klinker *et al.* [4] employ a pixel clustering algorithm which has been shown to work well in detecting brightness in images of plastic objects. Gershon *et al.* [5] and Lee *et al.* [6] use chromatic information for highlight identification. A similar approach is presented by Sato and Ikeuchi [7], who employ a so-called temporal-color space to extract the specular reflection and the body reflection. These previous approaches have produced good results, but they have requirements that limit their applicability such as the use of stereo or multiple-view systems, the previous knowledge of the scene, or the assumption of a homogeneous illumination, without considering the interreflections present in most typical real scenes.

In this paper, we develop an automatic system for the detection of highlights in images by means of the use of a two-dimensional (2-D) histogram of intensity and saturation signals from a three-dimensional (3-D) polar coordinate color representation. This representation allows us to obtain a specular reflectance map of the image. Once the specularities have been identified, they are eliminated from the image by applying a vectorial geodesic reconstruction algorithm, which has a low cost and avoids the oversimplification of the image.

In this paper, the two most important steps of the method proposed for brightness detection and elimination are described. In Section II, we present the color space used for the processing, together with the MS diagram developed to detect the specular reflectance. In addition, experimental results for the detection of brightness in real scenes are given. In Section III, we present the extension of the geodesic operations to color images. In Section IV, we develop a new connected vectorial filter for eliminating the highlights detected in Section II. This elimination and the parameters of the algorithm are presented in Section V. Finally, our conclusions are outlined in Section VI.

Manuscript received March 1, 2004; revised September 15, 2005. This paper was recommended by Guest Editors J. Salvador Sánchez, F. Pla, and D. Maravall.

The authors are with the Automatics, Robotics and Computer Vision Group, Department of Physics, Systems Engineering and Signal Theory, University of Alicante, 03690 Alicante, Spain (e-mail: fortiz@ua.es; fernando.torres@ua.es).

Digital Object Identifier 10.1109/TSMCC.2005.855424

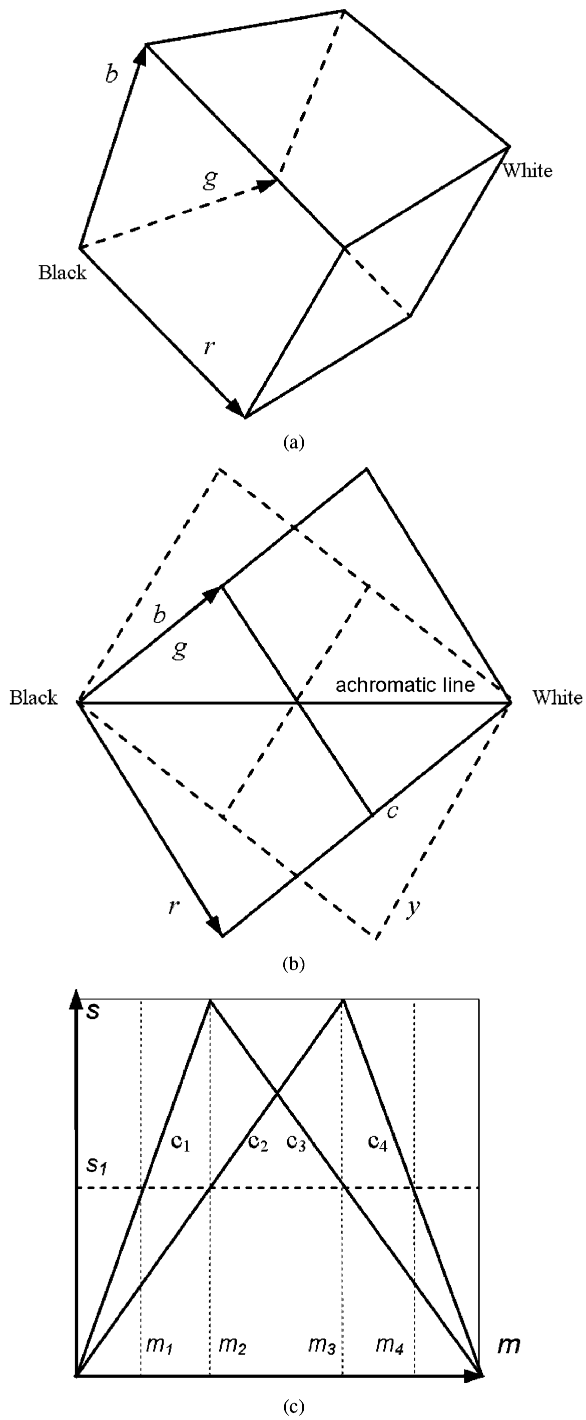

Fig. 1. RGB cube and its transformation in MS diagram. (a) 3-D projection. (b) 2-D opposite projections. (c) Shape and limits of MS diagram.

II. Color Spaces and MS Diagram

The color receptors of the human eye (cones) are more sensitive to the blue, green, and red zones of the spectrum, and the signals they emit are further processed in the brain's visual system. However, in the perception process, the human brain does not estimate the exact amounts of red, green, and blue in objects, but rather the basic attributes of color, such as intensity, hue, and saturation [8]–[10]. These attributes define the in-

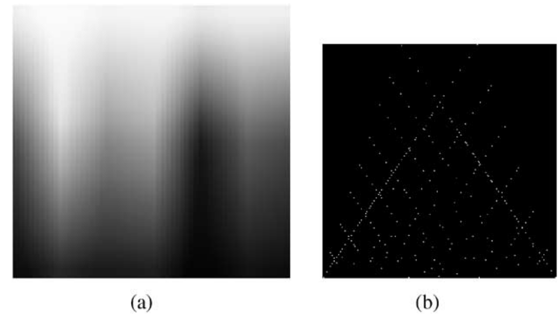

Fig. 2. (a) Synthetic chromatic image and (b) its MS diagram.

tuitive color systems Hue-Saturation-Intensity, Hue-Lightness-Intensity, Hue-Saturation-Value (HSI, HLS, HSV, etc.) which are widely used in image processing. They can be represented by a single system, which Levkowitz and Herman define as Generalized Lightness-Hue-Saturation (GLHS) [11], adapted for image processing by Serra's *L1-norme* [12]. We shall denote the intensity function by m, which is the mean of the r, g, and b values, where (r, g, b) are coordinates of the RGB color space [Fig. 1(a)], with $r \in [0, 255], g \in [0, 255]$ and $b \in [0, 255]$. As such, m corresponds to the l in the LHS-triangle model

$$m = \frac{1}{3}(r + g + b). \tag{1}$$

The m signal calculated is the normalization $(0 \leq m \leq 255)$ of the achromatic axes of the RGB cube. In Fig. 1(b), two opposite 2-D projections of the 3-D cube are observed. The value of s is given by Serra's *L1-norme* as

$$s = \begin{cases} \frac{1}{2}(2r - g - b) = \frac{3}{2}(r - m), & \text{if } (b + r) \geq 2g \\ \frac{1}{2}(r + g - 2b) = \frac{3}{2}(m - b), & \text{if } (b + r) < 2g. \end{cases} \tag{2}$$

A. MS Diagram

We propose to exploit the existing relation between m and s that permits the detection of specular reflections in a digital image, independently of the hue of the object in which the brightness appears [13]. Fig. 1(c) shows the MS diagram as the positive projection of all of the corners of the cube in a normalization of the achromatic line to the m signal.

The MS diagram is a grey image $f(m, s)$ in which each coordinate (m, s) indicates the quantity of the pixels in values of m and s of the original color image [14]

$$f(m, s) = \frac{\log(\mathrm{MS}(m, s))}{\max(\log(\mathrm{MS}(m, s)))} 255 \tag{3}$$

where $m \in [0, 255], s \in [0, 255]$ and $f(m, s) \in [0, 255]$. In Fig. 2, a synthetic color image and its corresponding MS diagram are shown. As can be seen, the maximum values of s along m are limited to the shape defined in Fig. 1(c).

B. Extraction of Specular Reflectance

It is known that the specularities in the chromatic image have values of high m and low $s, m \in [m_{\min}, m_{\max}], s \in [s_{\min}, s_{\max}]$, where $m_{\max} = 255$ and $s_{\min} = 0$. This represents

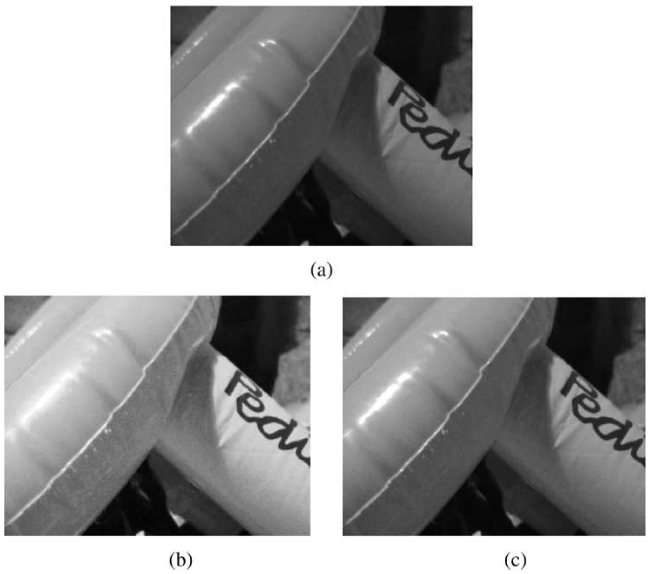

Fig. 3. Contrast enhancement of color image. (a) Chromatic real scene. (b) Contrast enhancement by histogram equalization. (c) Contrast enhancement by top hat contrast operator.

a given position of the MS diagram, precisely in the defined area under s_1 (saturation of primary colors G and B) and the projection of the corners c_3 and c_4 of the RGB cube. The achromatic axes zone could be considered as a highlight. This is partly true because it is only fulfilled for grayscale images. In color images, as m decreases, the brightness shows a similar color of surface (diffuse reflection) of the objects on which this brightness appears, approaching the c_3 and c_4 lines, whose definitions are

$$\begin{cases} c_3 = -\frac{3}{2}(m-255), & \forall m \in [m_3, m_{\max}] \\ c_4 = -3(m-255), & \forall m \in [m_4, m_{\max}] \end{cases} \quad (4)$$

where it is easily observed that $m_3 = (2/3)m_{\max}$ and $m_4 = (5/6)m_{\max}$. The value of $m_{\min}$ is calculated from c_3, such as

$$m_{\min} = \frac{2s_{\max} - 3m_{\max}}{-3}. \quad (5)$$

The $s_{\max}$ value is still to be calculated. An important consideration is that not all the images have the same dynamic range and, therefore, the m and s values of their specularities do not correspond with the positions of the MS diagram previously presented. The solution to this problem could be a contrast enhancement of the image by a histogram equalization of the m signal, but this is not the best solution, as it can sometimes cause an excessive increase in intensity and oversaturation, resulting in a false detection of objects, as if they were brightness. In order to avoid such inconveniences, we have opted for a neighborhood-based morphological contrast enhancement which considers the local features of the images. Specifically, m' is the result of a top hat contrast operator [15] defined as

$$m' = m + \mathrm{WTH}(m) - \mathrm{BTH}(m). \quad (6)$$

In Fig. 3, we show the difference between the contrast enhancement by histogram equalization and the morphological contrast operator that does not excessively increase the intensity of the image "life-saver" and is effective in the regions of mild specularities.

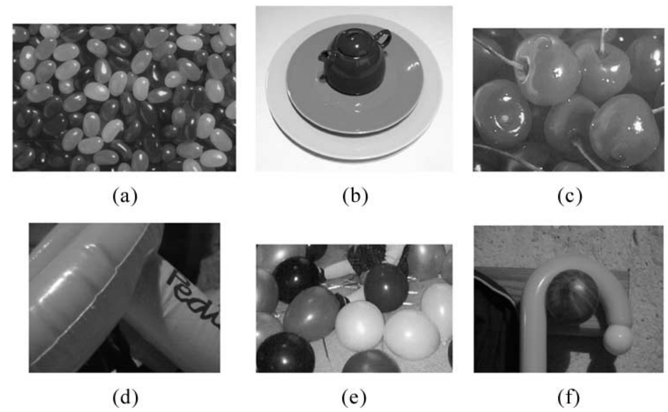

Fig. 4. Color images for empirical study using different types of materials. (a) Plastic in "color-beans." (b) Ceramics in "plates." (c) Fruit in "cherries." (d) Plastic in "life-saver." (e) Plastic in "balloons." (f) Wood in "umbrella."

This operation expels only the highlights from within the limits of the RGB cube. The result of the local enhancement by the top hat is that the specular reflectance pixels are positioned on the c_3 and c_4 lines in the MS diagram. These lines identify different specularities along their coordinates, from the most intense to the dullest. The optimum height for both lines (c_3 and c_4) can be determined experimentally. In the next section, we present the results of a study carried out on a set of real chromatic images that are quite representative of countless common materials (i.e., plastic, ceramics, fruit, wood, etc.), in which there are strong and weak reflectances. The images used in the study are shown in Fig. 4. The MS diagrams are presented in Fig. 5. In Fig. 6, we can see the pixels with saturation and intensity defined by the lines c_3 and c_4. As can be seen, all of the specularities have been detected. In some cases, such as "cherries" and "life-saver," just one line is sufficient, since all of the highlights are located on the same hue. Fig. 7 shows the evolution of the specularities detected when the saturation s is increased along c_3 and c_4. It is a logarithmic evolution where most of the bright pixels are located in maximum value of m and minimum s. The rest correspond to the transition from specular to diffuse reflection of the dichromatic refection model [1] in the surface of the objects. The graphs show that the detection of specularities stops, in all of the cases, at a maximum saturation of $s_{\max} = (m_{\max})/(10)$, and at higher values, no additional pixels in the image are detected as brightness. We obtained the same results with other images. It is now easy to calculate the value of $m_{\min}$ (5).

III. Mathematical Morphology and Color Geodsy

The definition of morphological operators needs a totally ordered complete lattice structure [16], [17]. The color pixels do not present, *a priori*, this structure, and it is necessary to impose an order relationship in the color space. Several studies have been carried out on the application of mathematical morphology to color images [18]–[21]. The approach most commonly adopted is based on the use of a lexicographical

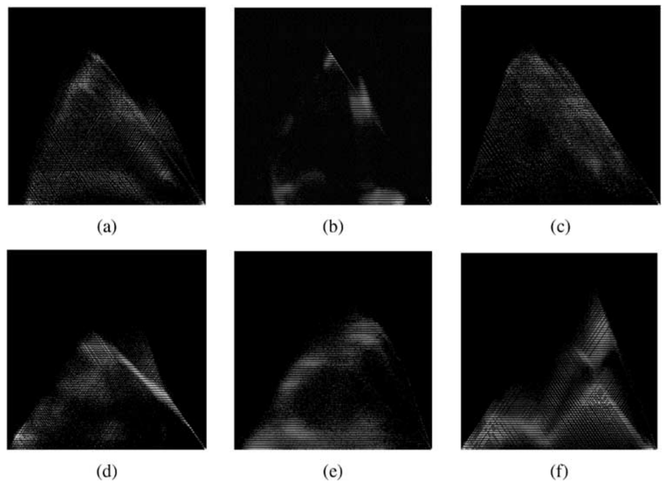

Fig. 5. MS diagrams of color images in Fig. 4. Highlights are present in the lines c_3 and c_4 of the diagrams.

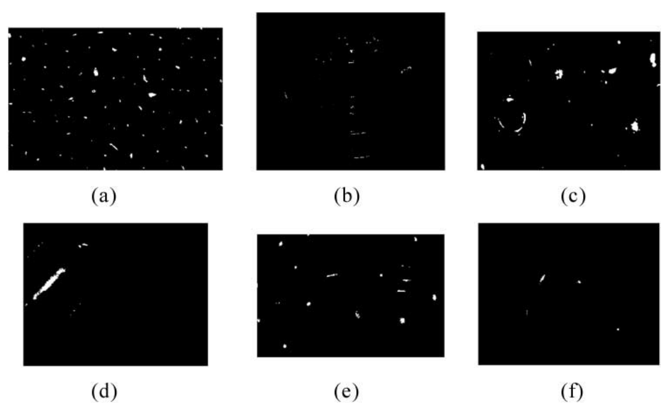

Fig. 6. Masks of brightness. Experimental results for real scenes in Fig. 4. The white points represent pixels of specular reflectance: (a) 347 in 192×128 of "color-beans." (b) 122 in 169×148 of "plates." (c) 237 in 164×124 of "cherries." (d) 218 in 165×128 of "life-saver." (e) 187 in 168×110 of "balloons." (f) 48 in 162×127 of "umbrella."

order, which imposes total order on the vectors. In this way, we avoid the false colors in an individual filtering of signals. Let $\mathbf{x} = (x_1, x_2, \ldots, x_n)$ and $\mathbf{y} = (y_1, y_2, \ldots y_n)$ be two arbitrary vectors $(\mathbf{x}, \mathbf{y} \in Z^n)$. An example of lexicographical order o_{lex}, will be

$$\mathbf{x} < \mathbf{y} \text{ if } \begin{cases} x_1 < y_1 \text{ or} \\ x_1 = y_1 \text{ and } x_2 < y_2 \text{ or} \\ x_1 = y_1 \text{ and } x_2 = y_2 \ldots \text{and} \ldots x_n < y_n. \end{cases} \tag{7}$$

On the other hand, it is important to define the color space in which operations are to be made. We use the normalized intuitive color space MSH (intensity, saturation, and hue). The preference or disposition of the components of the MSH in the lexicographical ordering depends on the application and the properties of the image. Ordering with intensity in the first position is the best way of preserving the contours of the objects in the image (lattice influenced by intensity). For our application, we employ this strategy. We define a lattice with a lexicographical order of $o_{\text{lex}} = (m \rightarrow s \rightarrow h)$ [19], [21]. As such, we put more emphasis on the intensity signal m. Afterward, we analyze the saturation. Next, we compare a hue distance value only if the pixels are colored.

A. Connected Vectorial Filters

Morphological filters by reconstruction have the property of suppressing details, preserving the contours of the remaining objects [22]–[24]. The use of these filters in color images requires an order relationship among the pixels of the image. For the vectorial morphological processing the lexicographical ordering, previously defined o_{lex}, will be used. The infimum $(\wedge_v)$ and supremum $(\vee_v)$ will be vectorial operators, and they will select pixels according to the order o_{lex} in the MSH generalized color space.

Once the orders have been defined, the morphological operators of reconstruction for color images can be generated and applied. An elementary geodesic operation is the geodesic dilation. Let $\boldsymbol{g}$ denote a marker color image and $\boldsymbol{f}$ a mask color image (if $o_{\text{lex}}(\boldsymbol{g}) \leq o_{\text{lex}}(\boldsymbol{f})$, then $\boldsymbol{g} \wedge_v \boldsymbol{f} = \boldsymbol{g}$). The vectorial geodesic dilation of size 1 of the marker image $\boldsymbol{g}$ with respect to the mask $\boldsymbol{f}$ can be defined as

$$\delta_{v\boldsymbol{f}}^{(1)}(\boldsymbol{g}) = \delta_v^{(1)}(\boldsymbol{g}) \wedge_v \boldsymbol{f} \tag{8}$$

where $\delta_v^{(1)}(\boldsymbol{g})$ is the vectorial dilation of size 1 of the marker image $\boldsymbol{g}$. This propagation is limited by the mask f.

The vectorial geodesic dilation of size n of a marker color image $\boldsymbol{g}$ with respect to a mask color image $\boldsymbol{f}$ is obtained by performing n successive geodesic dilations of $\boldsymbol{g}$ with respect to $\boldsymbol{f}$

$$\delta_{v_f}^{(n)}(g) = \delta_{v_f}^{(1)}\left[\delta_{v_f}^{(n-1)}(g)\right] \tag{9}$$

with $\delta_{v\boldsymbol{f}}^{(0)}(\boldsymbol{g}) = \boldsymbol{f}$.

Geodesic transformations of bounded images always converge after a finite number of iterations. The propagation of the marker image is impeded by the mask image. Morphological reconstruction of a mask image is based on this principle.

The vectorial reconstruction by dilation of a mask color image $\boldsymbol{f}$ from a marker color image $\boldsymbol{g}$, (both with $\mathrm{D}\boldsymbol{f} = \mathrm{D}\boldsymbol{g}$ and $\delta_{v\boldsymbol{f}}^{(n)}(\boldsymbol{g}) = \delta_{v\boldsymbol{f}}^{(n+1)}(\boldsymbol{g})$) can be defined as

$$R_{v\boldsymbol{f}}(\boldsymbol{g}) = \delta_{v\boldsymbol{f}}^{(n)}(\boldsymbol{g}) \tag{10}$$

where n is such that $\delta_{v\boldsymbol{f}}^{(n)}(\boldsymbol{g}) = \delta_{v\boldsymbol{f}}^{(n+1)}(\boldsymbol{g})$.

The vectorial reconstruction is an algebraic opening (increasing, antiextensive, and idempotent) only if all the operations between pixels respect the total order; in our case, the lexicographical order.

IV. Elimination of Specularities

To eliminate the highlights that were previously detected with the MS diagram, we use a new geodesic reconstruction filter. It is a vectorial opening by reconstruction (VOR) applied to the specular areas of the image and their surroundings. In this case, a new mask-image h represents the pixels of $\boldsymbol{f}$ with which we will be operating. The mask-image h is a dilation of the mask

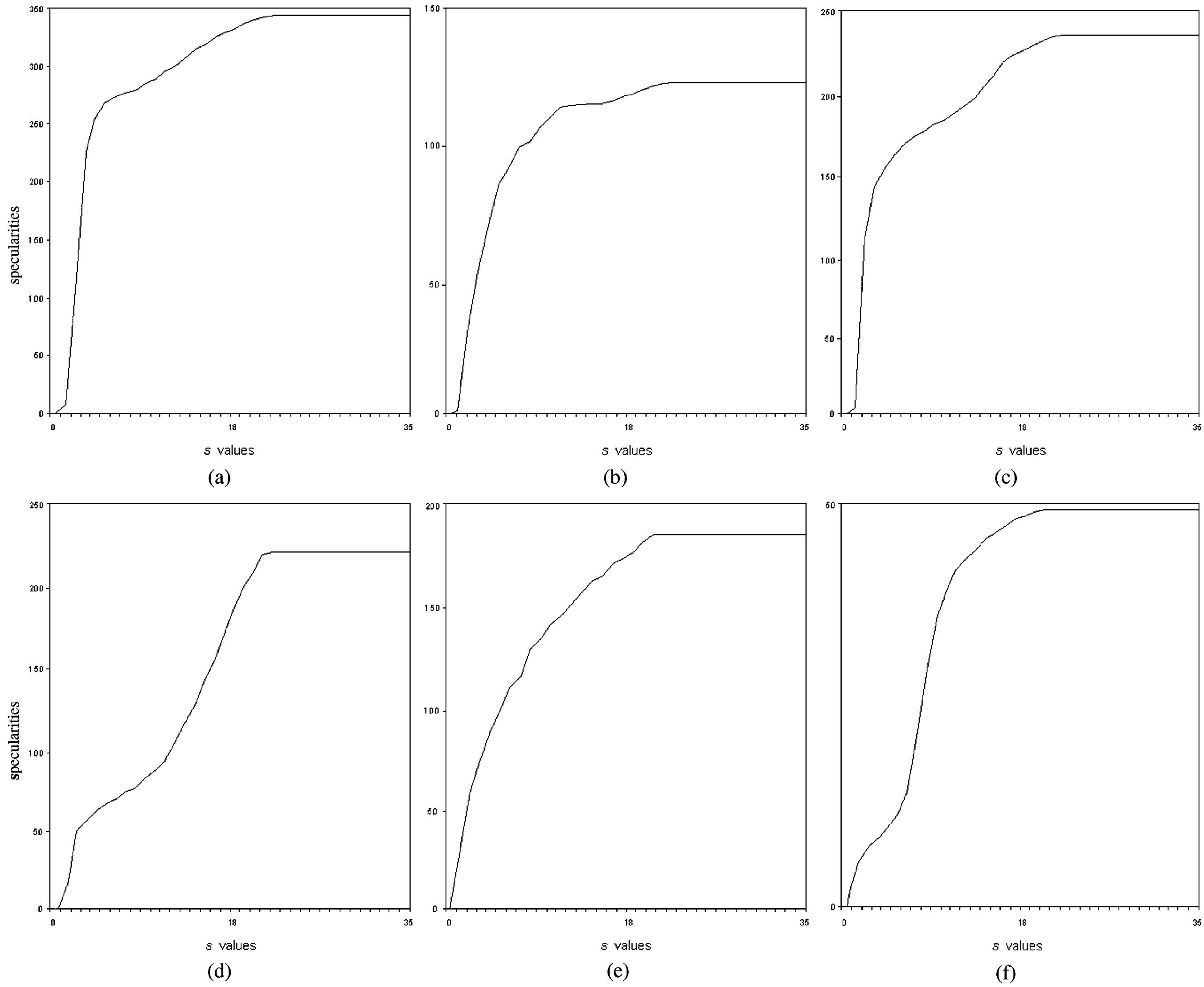

Fig. 7. Evolution of the specularities detected according to values of s. (a) "Color-beans." (b) "Plates." (c) "Cherries." (d) "Life-saver." (e) "Balloons." (f) "Umbrella."

of specularities (Fig. 6). Assuming that $D_h = D_f$, each pixel (x, y) has a value of $h(x, y) = \{0, 1\}$, where $h(x, y) = 1$ in the new areas of interest in the image.

In the VOR, $\boldsymbol{f}$ is first eroded. The eroded sets are then used as sets for a reconstruction of the original image. The new VOR is defined, taking into account the fact that, in this case, the operation will not affect all the pixels (x, y), but only those in which $h(x, y) = 1$

$$\gamma_{v_{\boldsymbol{f}},h}^{(n')} = \left\{ \delta_{v_{\boldsymbol{f}}}^{(n')} \left(\varepsilon_v^{(s)}(f) \right) \mid \forall f(x, y) \Rightarrow h(x, y) = 1 \right\} \quad (11)$$

where n' represents the successive iterations of the geodesic dilation, and the vectorial erosion of the opening by reconstruction is done with a structural element of size s, which is automatically obtained from the largest area of specular objects of Fig. 6. As such, the new local filter is a totally automatic method for brightness elimination. The vectorial erosion replaces highlight pixels (high o_{lex}) by the surroundings chromatic pixels (low o_{lex}). Next, the vectorial geodesic dilation (iterated until stability) reconstructs the color image without the recovering of the specularities. This is the same approach successfully used for the attenuation of the color objects in medical images [25], the Gaussian noise reduction [26], or filling the holes [27].

In this new operation, we avoid some of the main inconveniences of the geodesic reconstruction; i.e., the high cost of processing caused by the multiple iterations of the reconstruction, the oversimplification of the image [21], and the manual selection of the structural element of the operations.

The morphological function now operates only in the bright areas and their surrounding pixels. As such, the surrounding pixels replace the specular reflectance. This approach is an advance with respect to the brightness elimination by selection of area by means of color marker [28].

The main steps of the proposed method are summarized in Fig. 8.

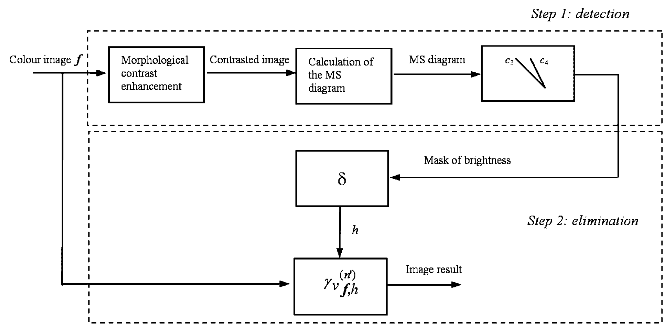

Fig. 8. Algorithm steps for the detection and elimination specular reflectance in color images.

TABLE I
PARAMETERS OF THE ALGORITHM

Color image	s	n	n'	Reduction of processing time (%)
Color-beans	5 (9x9)	59	17	57%
Umbrella	3 (7x7)	78	27	73%
Life-saver	4 (9x9)	89	21	76%
Plates	1 (3x3)	47	9	87%
Cherries	4 (9x9)	65	28	62%
Ballons	3 (7x7)	97	34	66%

V. RESULTS

We now present the results obtained from the application of our method for eliminating the specularities detected in the different real scenes in Fig. 4. For each experiment, we show the global vectorial color opening by reconstruction of the original image, and the new proposed filter which only operates in the bright areas that have previously been detected in the original image.

From the results obtained, the effectiveness of our method for the detection and elimination of specular reflectance can be observed. It must be emphasized that in the results obtained with the new filter, the oversimplification does not appear. In conventional connected filters, the size of the structuring element required for eliminating the specular reflectance causes a loss of detail in the images. These features can not be retrieved in the geodesic reconstruction. This has occurred in all the tested images of the experiment, and is more visible in the scenes of "plates," "cherries," "life-saver" and "balloons" [Fig. 9(c), (e), (g), and (i), respectively]. This undesirable effect does not appear with our algorithm, since the erosion and reconstruction only function in bright areas. Furthermore, as the function of the connected filters is restricted to specific areas in the image, the results are obtained at a much lower processing cost.

Details of algorithm parameters for the color images of this experiment can be observed in Table I. The size s of the structural element required in the vectorial erosion is automatically calculated from the masks of brightness in Fig. 6. The global vectorial geodesic dilation requires more iterations n (with a longer processing time) than the new operation n'. This reduction of time is important in the geodesic operations.

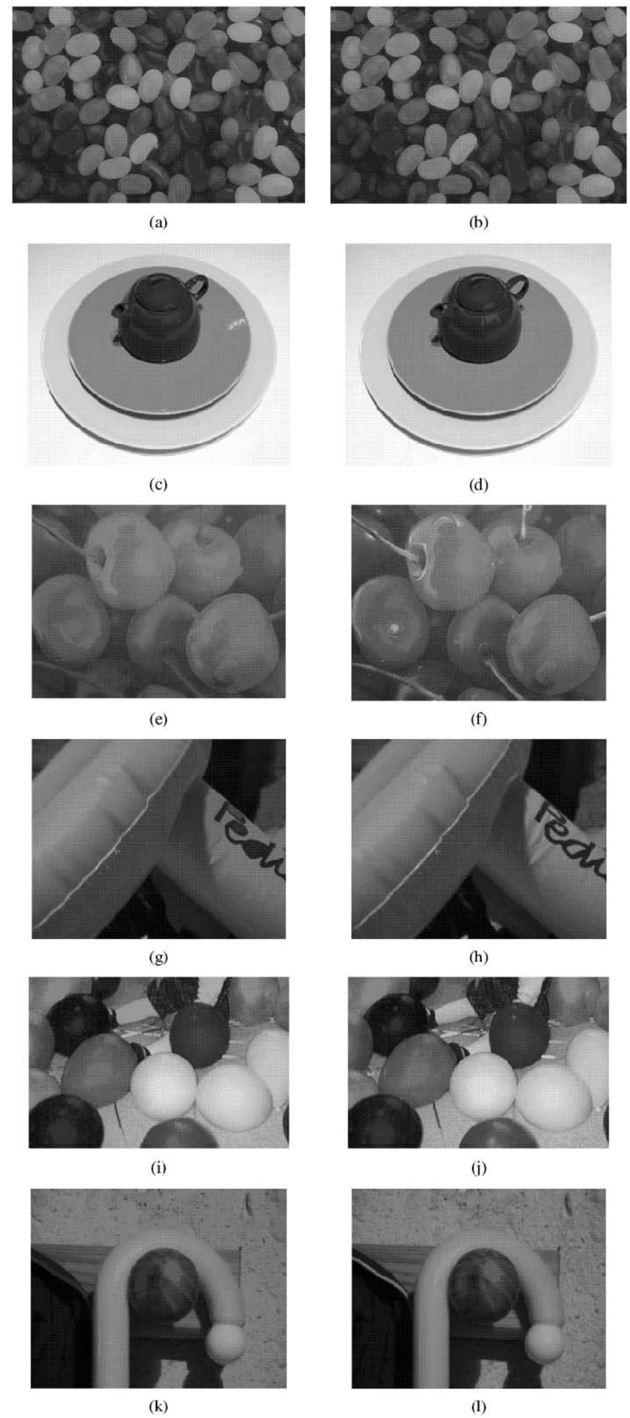

Fig. 9. Elimination of specular reflectance of real color images in Fig. 4 by means a global vectorial color opening by reconstruction (left column) and the results of our proposed method (right column).

VI. CONCLUSION

In this paper, we have presented a new method for the detection and elimination of specular reflectance in color images in order to allow a correct identification of objects in computer vision. We have show the effectiveness of the MS diagram in brightness detection. A detailed study has demonstrated that the specularities in real scenes appear in a given area of the MS diagram.

The use of a new connected vectorial filter allows us to eliminate the specular reflectance previously detected. This filter is an extension of the geodesic transformations of the mathematical morphology to color images. The possibility of eliminating brightness in color images without causing oversimplification has also been demonstrated. In addition, the elimination of brightness has been obtained automatically with a very low processing time, with respect to a global geodesic reconstruction. The detection and elimination of brightness is achieved independently of the material of the objects on which they appear, without any need of multiple view of the scenes.

Based on the success shown by these results, we are now working to improve our method for detecting and eliminating specularities. Specifically, in the highlight detection step, we are researching the effectiveness of using other color spaces based on polar coordinates. In the highlight elimination step, the objective is to reduce the processing time required for geodesic operations as much as possible.

ACKNOWLEDGMENT

This work was initiated by F. Torres during a stay at the Center of Mathematical Morphology (Fontainebleau) of the École National des Mines de Paris in 2002, invited by J. Serra.

REFERENCES

[1] S. A. Shafer, "Using color to separate reflection components," *Color Res. Appl.*, vol. 10, pp. 210–218, 1985.

[2] S. Lin, Y. Li, S. Kang, X. Tong, and H. Shum, "Diffuse-specular separation and depth recovery from image sequences," in *Lecture Notes in Computer Science*, vol. 2352, New York: Springer-Verlag, 2002.

[3] R. Bajcsy, S. Lee, and A. Leonardis, "Detection of diffuse and specular interface reflections and inter-reflections by color image segmentation," *Int. J. Comput. Vis.*, vol. 17, no. 3, pp. 241–272, 1996.

[4] G. Klinker, S. A. Shafer, and T. Kanade, "Image segmentation and reflection analysis through color," in *Appl. Artificial Intelligence VI, Proc. SPIE*, vol. 937, pp. 229–244, 1988.

[5] R. Gershon, A. D. Jepson, and J. K. Tsotsos, "Highlight identification using chromatic information," in *Proc. 1st Int. Conf. Computer Vision*, London, U.K., 1987, pp. 161–170.

[6] S. Lee and R. Bajcsy, "Detection of specularity using color and multiple views," *Image Vis. Comput.*, vol. 10, pp. 643–653, 1992.

[7] Y. Sato and K. Ikeuchi, "Temporal-color space analysis of reflection," in *Proc. IEEE Conf. Computer Vision and Pattern Recognition*, New York, 1993, pp. 570–576.

[8] H. Palus, "Representations of color images in different color spaces," in *The Color Image Processing Handbook*, S. Sangwine and R. Horne, Eds., London, U.K.: Chapman and Hall, pp. 67–90, 1998.

[9] G. Wyszecki and W. S. Stiles, *Color Science, Concepts and Methods, Quantitative Data and Formulas*, 2nd ed., New York: Wiley, 1982.

[10] K. N. Plataniotis and A. N. Venetsanopoulos, *Color Image Processing and Applications*. New York: Springer-Verlag, 2000.

[11] H. Levkowitz and G. Herman, "GLHS: A generalized lightness, hue and saturation color model," *Graph. Models Image Process.*, vol. 55, no. 4, pp. 271–285, 1993.

[12] J. Serra, "Espaces couleur et traitement d'images," Centre de Morphologie Math., École des Mines de Paris, Paris, France, Tech. Rep. N-34/02/MM, 2002.

[13] F. Torres, J. Angulo, and F. Ortiz, "Automatic detection of specular reflectance in color images using the MS diagram," in *Lecture Notes in Computer Science*, vol. 2756, pp. 132–139, New York: Springer-Verlag, 2003.

[14] J. Angulo, "Morphologie mathématique et indexation d'images couleur. Application á la microscopie en biomedicine," Ph.D. dissertation, Center of Math. Morphology, École des Mines de Paris, Paris, France, 2003.

[15] P. Soille, "A note on morphological contrast enhancement," École des Mines d'Alés-EERIE, Tech. Rep. RT-PS-001, 1997.

[16] J. Serra, *Image Analysis and Mathematical Morphology*. New York: Academic, 1982, vol. I.

[17] ——, *Image Analysis and Mathematical Morphology, Vol II: Theoretical Advances*. New York: Academic, 1988.

[18] M. Comer and E. Delp, "Morphological operations for color image processing," *J. Electron. Imaging*, vol. 8, no. 3, pp. 279–289, 1999.

[19] F. Ortiz, F. Torres, J. Angulo, and S. Puente, "Comparative study of vectorial morphological operations in different color spaces," in *Proc. SPIE, Intelligent Robots and Computer Vision XX*, vol. 4572, Boston, MA, 2001, pp. 259–268.

[20] A. Hanbury and J. Serra, "Morphological operators on the unit circle," *IEEE Trans. Image Process.*, vol. 10, no. 2, pp. 1842–1850, Feb. 2001.

[21] F. Ortiz, "Procesamiento morfológico de imágenes en color. Aplicación a la reconstrucción geodésica," Ph.D. dissertation, Dept. Phys. Syst. Eng. Signal Theory, Univ. Alicante, Alicante, Spain, 2002.

[22] L. Vicent, "Morphological grayscale reconstruction in image analysis: Applications and efficient algorithms," *IEEE Trans. Image Process.*, vol. 2, no. 2, pp. 176–201, Apr. 1993.

[23] J. Crespo, J. Serra, and R. Schafer, "Theoretical aspects of morphological filters by reconstruction," *Signal Process.*, vol. 47, pp. 201–225, 1995.

[24] P. Soille, *Morphological Image Analysis: Principles and Applications*. New York: Springer-Verlag, 1999.

[25] F. Ortiz, F. Torres, E. De Juan, and N. Cuenca, "Color mathematical morphology for neural image analysis," *Real Time Imaging*, vol. 8, no. 6, pp. 455–465, 2002.

[26] F. Ortiz, F. Torres, and P. Gil, "Gaussian noise elimination in colour images by vector-connected filters," in *Proc. 17th Int. Conf. Pattern Recognition*, vol. 4, Cambridge, U.K., 2004, pp. 807–810.

[27] P. Soille and C. Gratin, "An efficient algorithm for drainage networks extraction on DEMs," *J. Visual Commun. Image Represent.*, vol. 5, no. 2, pp. 181–189, 1994.

[28] F. Ortiz and F. Torres, "Vectorial morphological reconstruction for brightness elimination in colour images," *Real Time Imaging*, vol. 8, no. 6, pp. 379–387, 2004.

Francisco Ortiz was born in Melilla, Spain, in 1974. He received the Computer Science Engineer and Ph.D. degrees from the University of Alicante, Alicante, Spain, in 1998 and 2002, respectively.

He has been a full-time Professor in the Department of Physics, Systems Engineering and Signal Theory of the University of Alicante since 1999. He is involved in several research projects in collaboration with industry and the Spanish Government. His main research interests are industrial automatization, computer vision (specifically color systems), mathematical morphology, and new technologies for teaching. He has published several international papers.

Dr. Ortiz is a member of CEA-IFAC.

Fernando Torres (S'99–M'01) received the industrial engineer and Ph.D. degrees from Polytechnic University of Madrid (UPM), Madrid, Spain, in 1991 and 1995, respectively.

Since 1994, he has been at the University of Alicante, Alicante, Spain, as a Professor in control, robotics, and computer vision in the Department of Physics, Systems Engineering and Signal Theory. He is involved in several research projects in collaboration with industry and the Spanish Government. His main research interests include automatic visual inspection, robotics, manufacturing automation, visual servoing, morphological processing, and new technologies for teaching. He has published several international papers.

Dr. Torres is a member of the CEA-IFAC and the Spanish Image Analysis and Pattern Recognition Society.